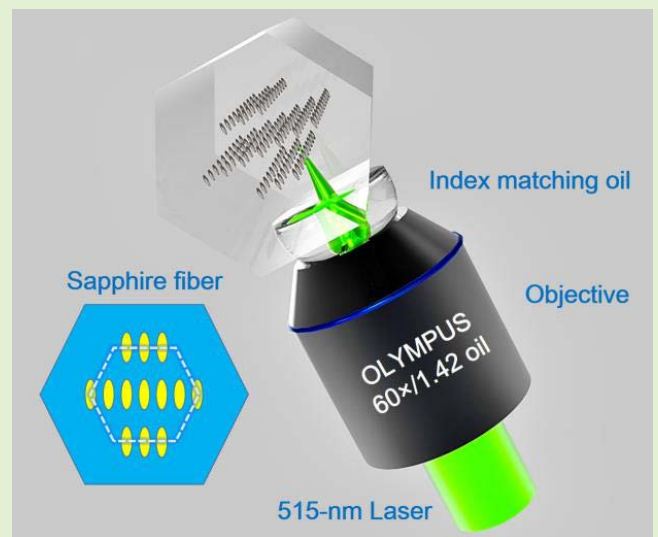


# Parallel-Integrated Sapphire Fiber Bragg Gratings Probe Sensor for High Temperature Sensing

Qi Guo, Zong-Da Zhang, Zhong-Ming Zheng, Xue-Peng Pan, Chao Chen<sup>ID</sup>, Zhen-Nan Tian<sup>ID</sup>, Qi-Dai Chen<sup>ID</sup>, Yong-Sen Yu<sup>ID</sup>, and Hong-Bo Sun<sup>ID</sup>, *Fellow, IEEE*

**Abstract**—This paper reports the fabrication of parallel integrated sapphire fiber Bragg gratings (SFBGs) probe sensor by the femtosecond laser point by point (PbP) method. The SFBGs probe sensor transmits optical signals through quartz multimode fiber, and takes an 8.5 mm sapphire fiber as the sensing probe, which can work stably for a long time at 1200 °C. This method can not only quickly prepare and obtain SFBGs with small bandwidth, but also obtain gratings with high reflectivity, which is about 15%. The mode field distribution in sapphire fibers with different lengths is studied by the beam quality analyzer. High-order modes are easily excited as the length of sapphire fibers increases. In addition, a spherical lens is prepared at the end of sapphire fiber, which effectively improve the signal-to-noise ratio (SNR) to 22 dB. The good spectral quality can still be maintained after holding at 1200 °C for 24 hours, and the temperature sensitivity can reach 30.19 pm/°C in the high temperature range, which is more than 2 times higher than that of quartz FBGs sensors. This parallel integrated SFBGs probe sensor overcomes the problems of doped quartz fiber element diffusion at high temperature and the instability of microstructure caused by material softening, and can be developed for long-term stable operation at 1200 °C high temperature and harsh environments.

**Index Terms**—Sapphire fiber Bragg gratings, mode field distribution, high-order modes, spherical lens.



Manuscript received January 13, 2022; revised February 3, 2022; accepted February 3, 2022. Date of publication February 7, 2022; date of current version March 14, 2022. This work was supported in part by the National Natural Science Foundation of China under Grant 62090064, Grant 91860140, Grant 61874119, and Grant 62131018; and in part by the Finance Science and Technology Project of Hainan Province under Grant ZDYF2020217. The associate editor coordinating the review of this article and approving it for publication was Prof. Carlos Marques. (Corresponding author: Yong-Sen Yu.)

Qi Guo, Zong-Da Zhang, Xue-Peng Pan, Zhen-Nan Tian, Qi-Dai Chen, and Yong-Sen Yu are with the State Key Laboratory of Integrated Optoelectronics, College of Electronic Science and Engineering, Jilin University, Changchun 130012, China (e-mail: yuys@jlu.edu.cn).

Zhong-Ming Zheng is with the Changchun Institute of Optics, Fine Mechanics and Physics, Chinese Academy of Sciences, Changchun 130033, China.

Chao Chen is with the State Key Laboratory of Luminescence and Applications, Changchun Institute of Optics, Fine Mechanics and Physics, Chinese Academy of Sciences, Changchun 130033, China, also with the Center of Materials Science and Optoelectronics Engineering, University of Chinese Academy of Sciences, Beijing 100049, China, and also with the Xiong'an Innovation Institute, Chinese Academy of Sciences, Xiong'an 071800, China.

Hong-Bo Sun is with the State Key Laboratory of Integrated Optoelectronics, College of Electronic Science and Engineering, Jilin University, Changchun 130012, China, and also with the State Key Laboratory of Precision Measurement Technology and Instruments, Department of Precision Instrument, Tsinghua University, Haidian, Beijing 100084, China.

Digital Object Identifier 10.1109/JSEN.2022.3149508

## I. INTRODUCTION

HIGH temperature and harsh environments exist widely in many fields such as industry and aerospace [1], [2]. How to realize accurate and fast physical quantity sensing and measurement in these extreme environments is an important research topic. Optical fiber sensors have incomparable advantages over electronic sensors, such as anti-electromagnetic interference and chemical corrosion resistance [3]–[5]. The measurement of physical quantities such as temperature, pressure, torsion, angle and refractive index can be achieved through fiber sensors [6]–[10]. The traditional ultraviolet laser grating preparation technology has been widely used in various optical fibers, especially in photosensitive polymer fibers [11]–[13]. However, this preparation technology usually requires that the fibers have photosensitivity. In addition, it is easy to be thermally erased at high temperature, which is difficult to be stably applied in high temperature environment. In addition, with the development and maturity of silicon-based process technology, the sensors prepared also provide new methods for monitoring the physical quantities of the surrounding environment [14], [15]. Femtosecond laser micro-nano processing technology has been proven to

induce permanent refractive index changes in any transparent material, which is independent of the photosensitivity and chemical composition of the material [16], [17]. This is due to the nonlinear effect caused by the interaction between the ultra-high peak power femtosecond laser and materials [18]–[21]. This technology provides an efficient method for producing high-temperature resistant fiber gratings. A long-term stable high temperature sensor in the temperature range of 1200 °C is urgently needed in high temperature and harsh environments such as engine combustion chamber monitoring, petroleum cracking and metal smelting [22].

Limited by the doping elements in quartz fiber, element diffusion will occur at high temperature [23], [24], which will lead to the change of effective refractive index of fiber guide mode and spectral drift. This limits the long-term stable application of doped quartz fiber gratings above 1000 °C [25]–[27]. Although the microstructure fiber made of pure quartz material has no doped elements, the porous structure of the microstructure fiber makes the preparation of gratings difficult [28], [29]. In addition, due to the limitation of quartz softening point, the structure of submicron gratings in quartz fiber is unstable at 1200 °C for a long time, which will reduce the spectral quality and reflectivity. If the fiber Bragg gratings are prepared in the crystal fiber with high melting point, the problems of unstable grating structure and diffusion of doped elements at high temperature can be well solved. Single crystal sapphire fiber is undoubtedly a good choice because of its ultra-high melting point (2053 °C) and excellent optical properties [30].

In this paper, we report the fabrication of parallel integrated SFBGs in an 8.5 mm sapphire fiber by the femtosecond laser PbP method. The sensor composed of the SFBGs sensing probe and the quartz fiber can work stably at 1200 °C for a long time. The SNR of the spectrum is effectively improved by making a spherical lens structure at the end of sapphire fiber. The sensor has excellent high temperature stability, high temperature sensitivity, and high preparation efficiency. It can take advantage of the short sapphire fiber to improve the stable application range of quartz fiber in high temperature and harsh environments.

## II. SENSOR FABRICATION AND PRINCIPLE

Figure 1 shows the mode field distribution of sapphire fiber end faces with different lengths tested by a beam quality analyzer (Ophir SP928). The 810 nm single-mode laser is first passed through the graded index multimode fiber (62.5/125  $\mu\text{m}$ ), and then passed into the sapphire fiber with the diameter of 60  $\mu\text{m}$  and the lengths of 5 cm, 25 cm, 50 cm and 100 cm, respectively. The multimode fiber and sapphire fiber are fused together by a fusion machine. If the length of sapphire fiber is short, the mode field is mainly distributed in the center of the fiber. As the length of sapphire fiber increases, more high-order modes are excited, and the mode field is gradually distributed to the edge of the fiber. This will disperse the mode field in the sapphire fiber and reduce the energy density of the optical field, which also leads to the low reflectivity of SFBGs prepared by the femtosecond laser PbP method.

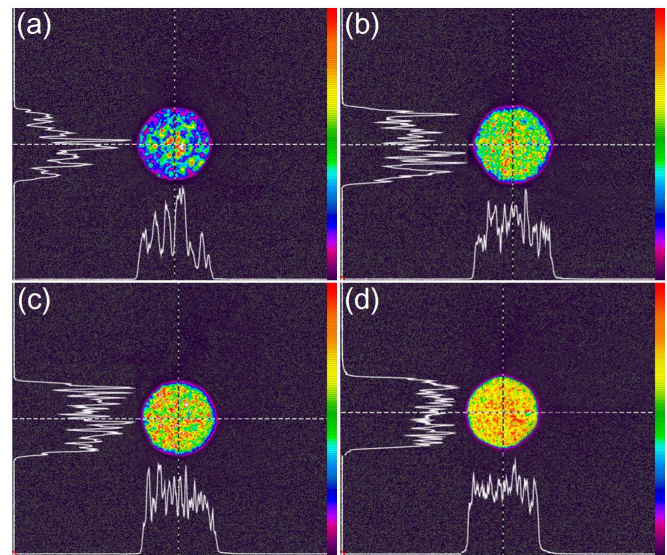
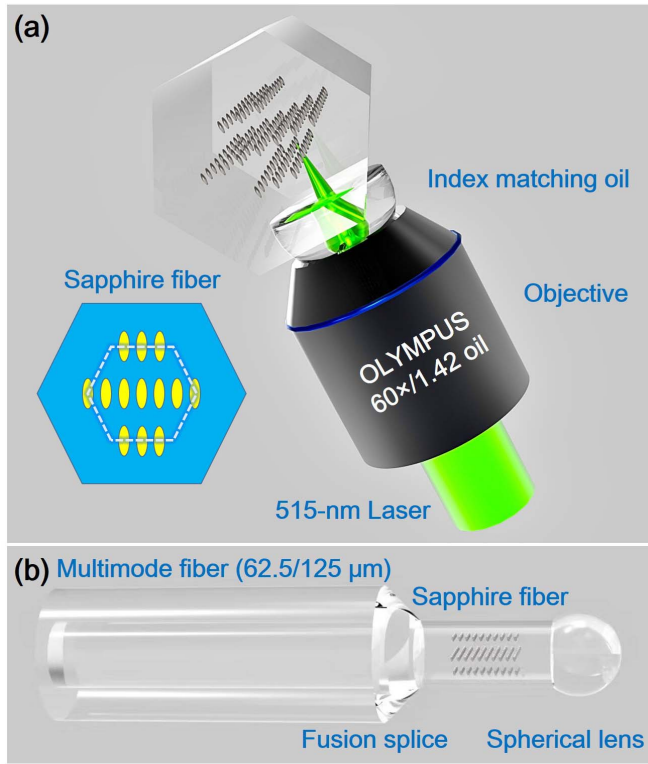


Fig. 1. The mode field distribution of 810 nm test light through sapphire fibers with lengths of 5 cm, 25 cm, 50 cm and 100 cm, respectively. The central region is the end profile of sapphire fiber, in which different colors represent different mode field intensity, and the edge curve represents the two-dimensional distribution of intensity.

Compared with line by line scanning method [31] or helical scanning method [32], the femtosecond laser PbP scanning method has the advantages of faster preparation speed and smaller FWHM [33]. The disadvantage is that the refractive index modulation region of single PbP scanning is small and the reflectivity of the prepared grating is low. Therefore, the SFBGs with high reflectivity and small FWHM can be prepared by PbP parallel-integrated method in short sapphire fiber. This method can expand the refractive index modulation region. In addition, the mode field distribution is concentrated in the center region of the short sapphire fiber, the excited high-order modes are less, and the periodic crosstalk between gratings is small, which is conducive to improving the reflectivity and reducing the FWHM.

Figure 2 (a) is a three-dimensional schematic diagram of preparing parallel-integrated SFBGs. The illustration is the two-dimensional distribution diagram of the end face of the prepared grating structure. The pulse width of the 515 nm femtosecond laser used is 290 fs, the single pulse energy is 160 nJ, and the repetition frequency is 400 Hz. The dotted line region is the main distribution region of short sapphire fiber mode field. By preparing SFBGs in parallel as shown in Fig. 2 (a), high preparation efficiency and coupling efficiency can be obtained. At the same time, there is no overlap between gratings and no crosstalk in grating period, which is conducive to quickly obtain SFBGs with high reflectivity and small bandwidth. The 515 nm femtosecond laser is focused into a 60  $\mu\text{m}$  sapphire fiber (MicroMaterials Inc.) through a oil-immersed objective lens (Olympus, 60 $\times$ /1.42). The single crystal sapphire fiber has a hexagonal lattice structure, and the femtosecond laser is focused vertically into the fiber from one side (A-Plane) of the sapphire fiber. The preparation of 7 parallel SFBGs in the middle layer is realized through PBP technology, and then 3 parallel SFBGs in the bottom layer are prepared. In order to obtain better grating quality





**Fig. 2.** (a) Schematic diagram of preparing parallel-integrated SFBGs. The illustration is the two-dimensional distribution diagram of the end face of the prepared grating structure. (b) Schematic diagram of high temperature fiber sensor integrated with quartz multimode fiber and sapphire fiber probe.

and symmetry, when preparing the top-layer SFBGs, it is necessary to rotate the sapphire fiber coaxially by 180 degrees, and then continue to prepare SFBGs by the same method as the bottom layer. Fig. 2(b) is a fiber high temperature sensor integrated with a quartz multimode fiber (62.5/125  $\mu\text{m}$ ) and a sapphire fiber probe. The quartz multimode fiber and sapphire fiber are fused by a fusion machine (Ericsson, FSU975), which ensures the stability of coupling efficiency and high temperature resistance. The discharge current and time are 10 mA and 1.5 s, respectively. By continuously optimizing the discharge current and discharge time, the fusion quality of quartz fiber and sapphire fiber is the best under this current and time, and good mechanical strength and fusion quality are obtained. Due to the large refractive index of sapphire fiber (1.746 @ 1550 nm), the Fresnel reflectivity at the end face is high, which will greatly reduce the spectral SNR.

In order to improve the spectral SNR, the spherical lens is prepared by high current discharge through a fusion splicer at the end of sapphire fiber, in which the discharge current is 16.5 mA and the discharge time is 2 s. The sapphire fiber is melted by electrode discharge heating and aggregated into an approximate spherical lens structure. The diameter of prepared spherical lens is larger than that of sapphire fiber, and more high-order modes will be further excited inside this spherical lens. The high-order mode excited is easy to scatter out, and some of the light will be reflected back into sapphire fiber. However, the optical power of this part is very small, so the

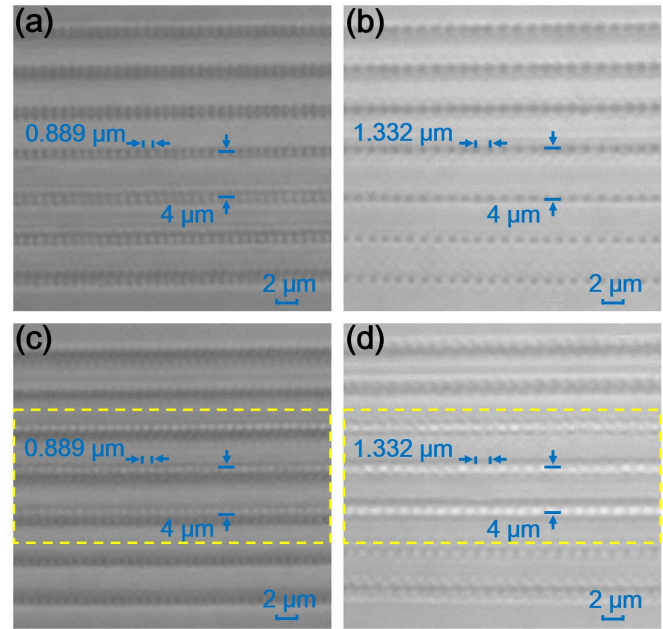


**Fig. 3.** (a) and (b) are micrographs of single-layer SFBGs prepared with grating spacing of 4  $\mu\text{m}$  and grating periods of 0.889  $\mu\text{m}$  and 1.332  $\mu\text{m}$ , respectively. Fig. 3. (c) and (d) are micrographs of three-layer SFBGs prepared with grating spacing of 4  $\mu\text{m}$  and grating periods of 0.889  $\mu\text{m}$  and 1.332  $\mu\text{m}$ , respectively.

spherical lens structure can significantly improve the SNR of the spectrum.

Figure 3 shows the micrographs of SFBGs with different periods and layers prepared by the femtosecond laser PbP method. Fig. 3 (a) and (b) are micrographs of single-layer SFBGs with grating periods of 0.889  $\mu\text{m}$  and 1.332  $\mu\text{m}$  and grating spacing of 4  $\mu\text{m}$ , respectively. Fig. 3 (c) and (d) are micrographs of the corresponding three-layer SFBGs. The interval between layers is 10  $\mu\text{m}$ , and multi-layer superposition will make the image unclear. The grating spacing of 4  $\mu\text{m}$  ensures no crosstalk and high discrimination between adjacent gratings.

### III. RESULTS AND DISCUSSION

Figure 4 (a) and (b) are the front and back ends of the sensor probe, and the illustration in Fig. 4 (b) is an enlarged view of the spherical lens area. After passing through the broadband light, part of the scattered light is clearly visible near the fusion point, grating and spherical lens regions. When broadband light passes through the spherical lens, most of the light will be scattered out. The overall length of the sapphire fiber probe is approximately 8.5 mm and the length of sapphire fiber at the front end of grating is 2 mm. The length of SFBG is 5 mm and the distance from the rear end of grating to spherical lens is 1.4 mm. The prepared spherical lens has a transverse diameter of 122  $\mu\text{m}$  and a longitudinal diameter of 148  $\mu\text{m}$ . Fig. 4 (c) shows the comparison of spectra before and after end face treatment, and the illustration is a partial enlargement of the spectrum in the wavelength range of 20 nm. By preparing a spherical lens at the end of sapphire fiber, the spectral SNR is greatly improved to 22 dB. The parallel

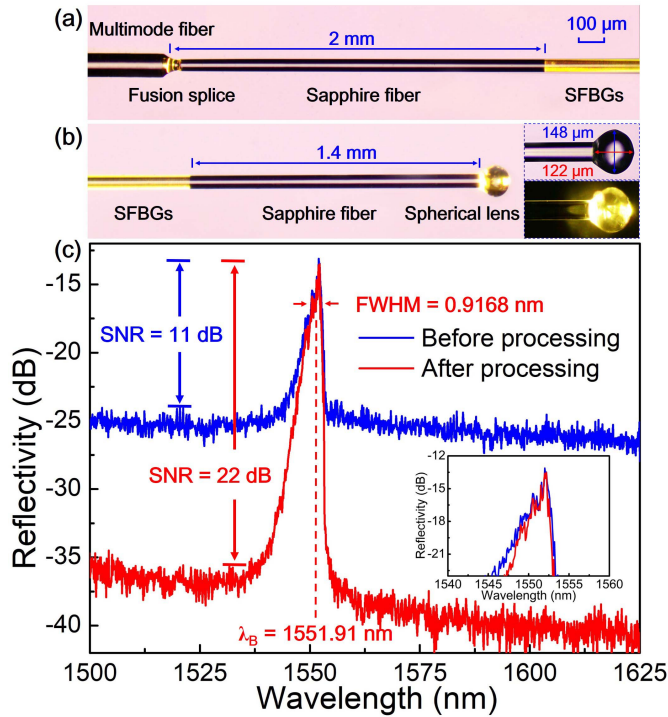


Fig. 4. (a) and (b) show the front and back ends of the sensor probe, and the illustration in Fig. 4(b) is an enlarged view of the spherical lens area. Fig. 4 (c) is the comparison of the spectrum before and after the end face treatment, and the illustration is a partial enlargement of the spectrum in the wavelength range of 20 nm.

integration of SFBGs prepared by femtosecond laser PbP method is helpful to increase the reflectivity of the grating and reduce the FWHM. The grating reflectivity is about 15%, and the FWHM is 0.9168 nm. If the FWHM is further significantly reduced, sapphire fiber can be coupled through single-mode fiber. However, due to the different mode field diameters of sapphire fiber and single-mode fiber, mode jump is easy to occur. This is also the reason why multimode fiber coupling sapphire fiber is used to prepare sensors.

By using high numerical aperture oil immersion lens to focus femtosecond laser, combined with PbP method, smaller period gratings can be prepared with high resolution. Fig. 5 is the spectral comparison of the prepared second-order and third-order SFBGs, and the illustration is the spectral comparison in the range of 20 nm. Compared with high-order SFBGs, low-order SFBGs with the same grating length have more cycles, higher diffraction efficiency and higher reflectivity, but this will also increase FWHM. The third-order SFBGs with smaller FWHM is selected in this experiment, which is conducive to improving the accuracy of spectral demodulation.

Remove the coating on the quartz fiber area of the sensor to be placed in the high-temperature area and wipe it clean with absolute ethanol. Put the sensor into a quartz tube sealed at one end. The inner diameter and outer diameter of the quartz tube used in this experiment are 1 mm and 2 mm. The purpose of this is to reduce the reaction between impurities and the surface of quartz fiber and sapphire fiber under high temperature and harsh environments, and thus reduce

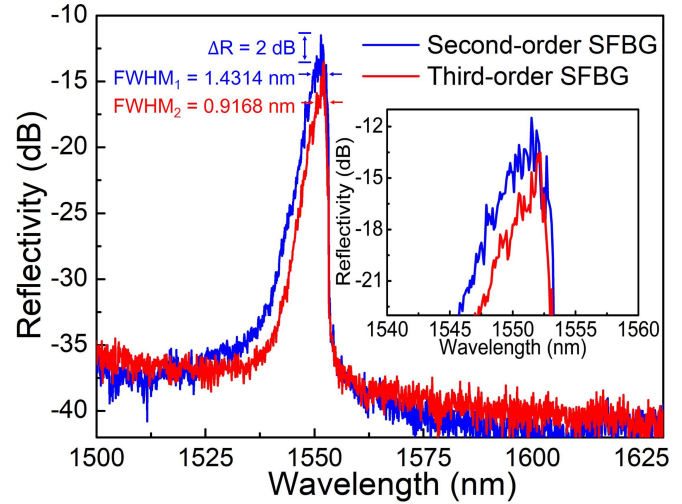


Fig. 5. (a) Spectral comparison of second-order and third-order SFBGs. The illustration shows a spectral comparison in the wavelength range of 20 nm.

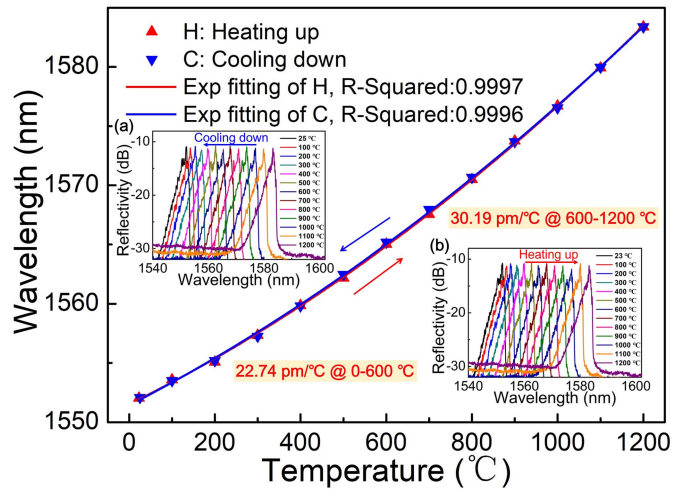


Fig. 6. The quadratic fitting curve of Bragg wavelength and temperature during the temperature cycling test from room temperature to 1200 °C. The illustration shows the variation of reflection spectra with temperature during cooling process (a) and heating process (b).

the performance of the sensor. Place the sensor in a high-temperature furnace, anneal it at 1000 °C for 3 hours, then cool it to room temperature to repeat the temperature cycle test. The maximum temperature is tested to 1200 °C, the temperature test interval is 100 °C, and each temperature point is held for 30 minutes. Fig. 6 is a quadratic fitting curve of Bragg wavelength and temperature during a temperature cycling test from room temperature to 1200 °C. The illustration shows the variation of reflection spectra with temperature during cooling process (a) and heating process (b). The quadratic fitting curve expression is:  $\lambda = A + B \cdot T + C \cdot T^2$ . The fitting parameters  $A$ ,  $B$  and  $C$  are 1551.52022, 0.01785 and  $7.31204 \times 10^{-6}$ , respectively. The temperature sensitivity of 22.74 pm/°C (@0-600 °C) and 30.19 pm/°C (@600-1200 °C) can be obtained by piecewise linear fitting of different temperature ranges. This is also one of the advantages of using sapphire fiber as sensing probe to obtain high temperature sensitivity.

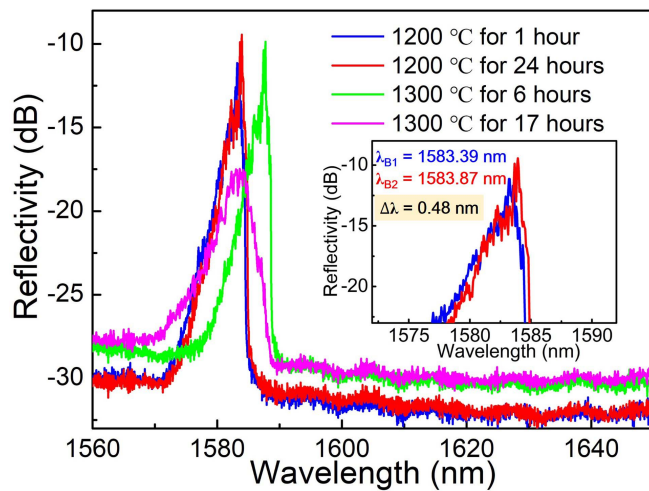


Fig. 7. Spectral comparison of long-time temperature stability test at 1200 °C and 1300 °C. The illustration is a comparison of spectral stability in the wavelength range of 20 nm at 1200 °C.

In order to further explore the long-term high temperature stability of the sensor, comparing the spectra of the sensor at 1200 °C for 24 hours and 1 hour, there is no obvious shift in the reflection spectra. The spectra remains relatively stable when the temperature rises to 1300 °C and remains for 6 hours. When the temperature is kept for 17 hours, the spectrum quality has obviously decreased. Fig. 7 shows the long-time spectral comparison at 1200 °C and 1300 °C, and the illustration shows the long-time spectral comparison in the wavelength range of 20 nm and holding at 1200 °C for 1 hour and 24 hours. Although the internal grating structure of sapphire fiber can remain stable at 1300 °C for a long time, the quartz softens obviously at this temperature, and the coupling region between quartz fiber and sapphire fiber changes, resulting in the reduction of coupling efficiency and the deterioration of spectrum. The long-time stability experiment shows that this sensor can work at 1200 °C for a long time and 1300 °C for a short time.

#### IV. CONCLUSION

In conclusion, we have prepared the three-layer parallel SFBGs with a 5 mm grating length in an 8.5 mm sapphire fiber by the femtosecond laser PbP method. The SFBGs probe and quartz multimode fiber constitute a fiber high temperature sensor, which can work stably at 1200 °C for a long time and 1300 °C for a short time. In order to reduce the problem of low SNR caused by Fresnel reflection, we fabricated a spherical lens on the sapphire fiber end face, which can effectively improve the SNR to 22 dB. In addition, due to the high thermal optical coefficient of sapphire material, the temperature sensitivity can reach 30.19 pm/°C in the high temperature range, which is more than 2 times higher than that of quartz FBGs sensors. The sensor overcomes the problems of doped quartz fiber element diffusion at high temperature and the instability of the microstructure caused by material softening, and can work stably in 1200 °C high temperature and harsh environments.

#### REFERENCES

- [1] B. Wang, Y. Niu, S. Zheng, Y. Yin, and M. Ding, "A high temperature sensor based on sapphire fiber Fabry-Pérot interferometer," *IEEE Photon. Technol. Lett.*, vol. 32, no. 2, pp. 89–92, Jan. 15, 2020.
- [2] Z. Shao *et al.*, "All-sapphire-based fiber-optic pressure sensor for high-temperature applications based on wet etching," *Opt. Exp.*, vol. 29, no. 3, pp. 4139–4146, 2021.
- [3] D. W. Lai *et al.*, "Design and validation of a miniature fiber Bragg grating-enabled high-sensitivity torque sensor," *IEEE Sensors J.*, vol. 21, no. 18, pp. 20027–20035, Sep. 2021.
- [4] M. Dai *et al.*, "Fiber optic temperature sensor with online controllable sensitivity based on Vernier effect," *IEEE Sensors J.*, vol. 21, no. 19, pp. 21555–21563, Oct. 2021.
- [5] M. Zou *et al.*, "Fiber-tip polymer clamped-beam probe for high-sensitivity nanoforce measurements," *Light, Sci. Appl.*, vol. 10, no. 1, pp. 1–12, Aug. 2021.
- [6] A. Leal-Junior, A. Frizera, C. Díaz, C. Marques, M. Ribeiro, and M. J. Pontes, "Material features based compensation technique for the temperature effects in a polymer diaphragm-based FBG pressure sensor," *Opt. Exp.*, vol. 26, no. 16, pp. 20590–20602, 2018.
- [7] A. G. Leal, Jr., *et al.*, "Polymer optical fiber for angle and torque measurements of a series elastic actuator's spring," *J. Lightw. Technol.*, vol. 36, no. 9, pp. 1698–1705, May 1, 2018.
- [8] A. Leal-Junior *et al.*, "Strain, temperature, moisture, and transverse force sensing using fused polymer optical fibers," *Opt. Exp.*, vol. 26, no. 10, pp. 12939–12947, May 2018.
- [9] A. Leal-Junior *et al.*, "Simultaneous measurement of axial strain, bending and torsion with a single fiber Bragg grating in CYTOP fiber," *J. Lightw. Technol.*, vol. 37, no. 3, pp. 971–980, Feb. 1, 2019.
- [10] A. G. Leal-Junior *et al.*, "Quasi-distributed torque and displacement sensing on a series elastic actuator's spring using FBG arrays inscribed in CYTOP fibers," *IEEE Sensors J.*, vol. 19, no. 11, pp. 4054–4061, Jun. 2019.
- [11] C. Broadway, R. Min, A. G. Leal-Junior, C. Marques, and C. Caucheteur, "Toward commercial polymer fiber Bragg grating sensors: Review and applications," *J. Lightw. Technol.*, vol. 37, no. 11, pp. 2605–2615, Jun. 1, 2019.
- [12] C. Marques *et al.*, "Advances on polymer optical fiber gratings using a KrF pulsed laser system operating at 248 nm," *Fibers*, vol. 6, no. 1, p. 13, 2018.
- [13] C. A. F. Marques *et al.*, "Fast and stable gratings inscription in POFs made of different materials with pulsed 248 nm KrF laser," *Opt. Exp.*, vol. 26, no. 2, pp. 2013–2022, Jan. 2018.
- [14] K. Xu, Y. Chen, T. A. Okhai, and L. W. Snyman, "Micro optical sensors based on avalanche silicon light-emitting devices monolithically integrated on chips," *Opt. Mater. Exp.*, vol. 9, no. 10, pp. 3985–3997, Oct. 2019.
- [15] K. Xu, "Silicon electro-optic micro-modulator fabricated in standard CMOS technology as components for all silicon monolithic integrated optoelectronic systems," *J. Micromech. Microeng.*, vol. 31, no. 5, May 2021, Art. no. 054001.
- [16] J. Thomas, C. Voigtländer, R. G. Becker, D. Richter, A. Tünnermann, and S. Nolte, "Femtosecond pulse written fiber gratings: A new avenue to integrated fiber technology," *Laser Photon. Rev.*, vol. 6, no. 6, pp. 709–723, 2012.
- [17] Z.-Z. Li *et al.*, "O-FIB: Far-field-induced near-field breakdown for direct nanowriting in an atmospheric environment," *Light, Sci. Appl.*, vol. 9, no. 1, pp. 1–7, Mar. 2020.
- [18] P. S. Salter and M. J. Booth, "Adaptive optics in laser processing," *Light, Sci. Appl.*, vol. 8, no. 1, pp. 1–16, Nov. 2019.
- [19] X. Wang, H. Fang, F. Sun, and H. Sun, "Laser writing of color centers," *Laser Photon. Rev.*, vol. 16, no. 1, Jan. 2022, Art. no. 2100029.
- [20] Y. Zhao, Y. Yang, and H.-B. Sun, "Nonlinear meta-optics towards applications," *Photonix*, vol. 2, no. 1, p. 3, Apr. 2021.
- [21] X. Li and Y. Guan, "Theoretical fundamentals of short pulse laser-metal interaction: A review," *Nanotechnol. Precis. Eng.*, vol. 3, no. 3, pp. 105–125, Sep. 2020.
- [22] X. Z. Xu *et al.*, "Multi-layer, offset-coupled sapphire fiber Bragg gratings for high-temperature measurements," *Opt. Lett.*, vol. 44, no. 17, pp. 4211–4214, Sep. 2019.
- [23] C. Zhu, R. E. Gerald, and J. Huang, "Progress toward sapphire optical fiber sensors for high-temperature applications," *IEEE Trans. Instrum. Meas.*, vol. 69, no. 11, pp. 8639–8655, Nov. 2020.
- [24] B. Liu *et al.*, "Sapphire-fiber-based distributed high-temperature sensing system," *Opt. Lett.*, vol. 41, no. 18, pp. 4405–4408, 2016.



- [25] T. Wang *et al.*, "Single crystal fibers: Diversified functional crystal material," *Adv. Fiber Mater.*, vol. 1, nos. 3–4, pp. 163–187, Dec. 2019.
- [26] Z. Wang *et al.*, "High temperature strain sensing with alumina ceramic derived fiber based Fabry–Pérot interferometer," *Opt. Exp.*, vol. 27, no. 20, pp. 27691–27701, Sep. 2019.
- [27] B. A. Wilson *et al.*, "Modeling of the creation of an internal cladding in sapphire optical fiber using the  ${}^6\text{Li}(n,\alpha)^3\text{H}$  reaction," *J. Lightw. Technol.*, vol. 36, no. 23, pp. 5381–5387, Dec. 1, 2018.
- [28] S. C. Warren-Smith *et al.*, "Temperature sensing up to 1300 °C using suspended-core microstructured optical fibers," *Opt. Exp.*, vol. 24, no. 4, pp. 3714–3719, Feb. 22, 2016.
- [29] A. Cusano, D. Paladino, and A. Iadicicco, "Microstructured fiber Bragg gratings," *J. Lightw. Technol.*, vol. 27, no. 11, pp. 1663–1697, Jan. 1, 2009.
- [30] X. Yu, S. Wang, J. Jiang, K. Liu, Z. Wu, and T. Liu, "Self-filtering high-resolution dual-sapphire-fiber-based high-temperature sensor," *J. Lightw. Technol.*, vol. 37, no. 4, pp. 1408–1414, Feb. 15, 2019.
- [31] X. Xizhen *et al.*, "Sapphire fiber Bragg gratings inscribed with a femtosecond laser line-by-line scanning technique," *Opt. Lett.*, vol. 43, no. 19, pp. 4562–4565, 2018.
- [32] Q. Guo *et al.*, "Femtosecond laser inscribed helical sapphire fiber Bragg gratings," *Opt. Lett.*, vol. 46, no. 19, pp. 4836–4839, Oct. 2021.
- [33] S. Yang, D. Hu, and A. Wang, "Point-by-point fabrication and characterization of sapphire fiber Bragg gratings," *Opt. Lett.*, vol. 42, no. 20, pp. 4219–4222, 2017.

**Qi Guo** received the B.S. degree from the College of Electronic Science and Engineering, Jilin University, China, in 2016, where he is currently pursuing the Ph.D. degree. His current research interests include theory of fiber gratings and fabrication of fiber gratings and the interaction of femtosecond laser and material.

**Zong-Da Zhang** received the B.S. degree from the College of Electronic Science and Engineering, Jilin University, China, in 2012, where he is currently pursuing the Ph.D. degree. His current research interests include femtosecond laser micronano machining and diamond color center.

**Zhong-Ming Zheng** received the M.S. degree from the College of Electronic Science and Engineering, Jilin University, China, in 2018. He works as an Engineer at the Changchun Institute of Optics, Fine Mechanics and Physics, Chinese Academy of Sciences, Changchun, China. His current research interests include high-energy laser diffraction components and holographic gratings.

**Xue-Peng Pan** received the B.S. degree from the College of Electronic Science and Engineering, Jilin University, China, in 2017, where he is currently pursuing the Ph.D. degree. His current research interests include theory of fiber gratings and fabrication of fiber gratings and the interaction of femtosecond laser and material.

**Chao Chen** received the B.S., M.S., and Ph.D. degrees in electronics science and technology from Jilin University, Changchun, China, in 2005, 2010, and 2014, respectively. He is currently an Associate Professor with the State Key Laboratory of Luminescence and Application, Changchun Institute of Optics, Fine Mechanics and Physics, Chinese Academy of Sciences, Changchun. His current research interests include narrow linewidth semiconductor laser, hybrid integrated laser, micro-nano integrated photonic devices, and optical fiber sensing.

**Zhen-Nan Tian** received the B.S. and M.S. degrees from the College of Physics in 2011 and 2014, respectively, and the Ph.D. degree in electronics science and technology from Jilin University, Changchun, China, in 2017. He was a Postdoctoral Researcher with the Politecnico di Milano, Italy, from 2019 to 2020. He is currently an Associate Professor with the State Key Laboratory of Integrated Optoelectronics, Jilin University. His current research interests include femtosecond laser microfabrication, micro-optics, integrated optoelectronic devices, and integrated quantum chip.

**Qi-Dai Chen** received the B.S. degree in physics from the University of Science and Technology of China, Anhui, China, in 1998, and the Ph.D. degree in plasma physics from the Institute of Physics, CAS, Beijing, China, in 2004. He worked as a JST Postdoctoral Researcher with the Department of Physics, Osaka City University, Japan, from 2005 to 2006, and then as an Associate Professor with the College of Electronic Science and Engineering, Jilin University, China. In 2011, he was promoted as a Full Professor. His research interests include laser nanofabrication technology for micro-optics, semiconductor laser beam shaping, and sub-wavelength anti-reflective microstructure. So far, he has published more than 250 scientific papers in the above fields, which have been cited for over 8000 times according to ISI search report.

**Yong-Sen Yu** received the Ph.D. degree from the College of Electronic Science and Engineering, Jilin University, China, in 2005. In 2019, he went to South Korea University as a Visiting Scholar for one year. He is currently a Full Professor with the College of Electronics Science and Engineering, Jilin University. His research interests include femtosecond laser micronano machining, fiber gratings, and optical fiber sensors.

**Hong-Bo Sun** (Fellow, IEEE) received the B.S. and Ph.D. degrees in electronics from Jilin University, Changchun, China, in 1992 and 1996, respectively. He worked as a Postdoctoral Researcher at the Satellite Venture Business Laboratory, University of Tokushima, Japan, from 1996 to 2000, and then as an Assistant Professor with the Department of Applied Physics, Osaka University, Japan. In 2004, he was promoted as a Full Professor (a Changjiang Scholar) with Jilin University, Changchun. Since 2017, he has been working at Tsinghua University, Beijing. His research interests include the ultrafast optoelectronics, particularly on laser nanofabrication and ultrafast spectroscopy: fabrication of various micro-optical, microelectronic, micromechanical, micro-optoelectronic, microfluidic components and their integrated systems at nanoscale, and exploring ultrafast dynamics of photons, electrons, phonons, and surface plasmons in solar cells, organic light-emitting devices, and low-dimensional quantum systems at femtosecond timescale. So far, he has published more than 350 scientific papers in the above fields, which have been cited for more than 12 000 times according to ISI search report. In 2017, he was selected as an OSA Fellow. He is currently the Topical Editor of *Optics Letters* (OSA), *Light: Science and Applications* (Nature Publishing Group), and *Chinese Science Bulletin* (Springer). He is an Editorial Advisory Board Member of *Nanoscale* (RSC) and *Display and Imaging* (Old City Publishing).